1650 *J. Phys. Chem. A* **2005,** *109,* 1650−1661

Conformational Stabilities of 1,1-Dicyclopropylethene Determined from Variable-Temperature Infrared Spectra of Xenon Solutions and ab Initio Calculations

James R. Durig,*,[‡] Chao Zheng,[‡,†] Gamil A. Guirgis,[§] and Charles J. Wurrey[‡]

Department of Chemistry, University of Missouri−Kansas City, 5100 Rockhill Road,
Kansas City, Missouri 64110, and Department of Chemistry & Biochemistry, College of Charleston,
Charleston, South Carolina 29424

Received: September 13, 2004; In Final Form: December 8, 2004

The infrared (3200−40 cm^{-1}) spectra of gaseous and solid 1,1-dicyclopropylethene, (c-C_3H_5)$_2$C═CH$_2$, along with the Raman (3200−40 cm^{-1}) spectra of liquid and solid phases, have been recorded. The major trans-gauche (C═C bond trans to one ring with the other ring rotated about 60° from the C═C bond, trivial C_1 symmetry) and gauche-gauche (the two three-membered rings rotated oppositely about 60° from the C═C bond, C_2 symmetry) rotamers have been confidently identified in the fluid phases, but no definitive spectroscopic evidence was found for the gauche-gauche′ form (the two three-membered rings rotated to the same side about 60° from the C═C bond, C_s symmetry), which is calculated to be present in no more than 6% at ambient temperature. Variable-temperature (−55 to −100 °C) studies of the infrared spectra of the sample dissolved in liquid xenon have been carried out. Utilizing six different combinations of pairs of bands from the C_1 and C_2 conformers, the average enthalpy difference between these two has been determined to be 146 ± 30 cm^{-1} (1.75 ± 0.36 kJ·mol^{-1}), with the C_1 form more stable. Given statistical weights of 2:1:1 respectively for the C_1, C_2, and C_s forms, it is estimated that there are 75 ± 2% C_1 and 19 ± 1% C_2 conformers present at ambient temperature. By utilizing predicted frequencies, infrared intensities, Raman activities, and band envelopes from scaled MP2(full)/6-31G(d) ab initio calculations, a complete vibrational assignment is made for the C_1 form and a number of fundamentals of the C_2 conformer have been identified. The structural parameters, dipole moments, and conformational stabilities have been obtained from ab initio calculations at the level of Hartree−Fock (RHF), the perturbation method to second order with full electron correlation (MP2(full)), and hybrid density functional theory (DFT) by the B3LYP method with a variety of basis sets. The predicted conformational stabilities from the MP2 calculations with relatively large basis sets are consistent with the experimental results. Structural parameters are estimated from the MP2(full)/6-311+G(d,p) predictions which are compared to the previously reported electron diffraction parameters. These experimental and theoretical results are compared to the corresponding quantities of some similar molecules.

Introduction

The monosubstituted methylcyclopropane molecules have been of interest to structural chemists and physicists for many years since there is the possibility of three different conformers, i.e., cis (syn), trans (anti), and gauche, being the most stable form. For example, cyclopropyl carboxaldehyde (c-C_3H_5CHO) has the cis and trans conformers[1−5] as the two stable forms, while for the isoelectronic vinylcyclopropane (c-C_3H_5CH═CH$_2$) molecule the two stable conformers[6−14] are the trans and the two equivalent gauche forms with the trans form reported[13] to be more stable with an enthalpy difference of 500 ± 50 cm^{-1} (5.98 ± 0.60 kJ·mol^{-1}). Whether vinylcyclopropane has a stable cis form has not been thoroughly investigated, although if this conformer does exist it must be in very small abundance at ambient temperature. Nevertheless, it is clear that there are significant differences in the conformational stabilities of monosubstituted vinyl and carbonyl cyclopropanes.

As a continuation of our studies of the conformational stabilities of substituted cyclopropanes, we initiated a vibrational and theoretical investigation of 1,1-dicyclopropylethene (c-(C_3H_5)$_2$C═CH$_2$) with particular interest for comparison with the corresponding ketone, dicyclopropyl ketone (c-(C_3H_5)$_2$C═O).[15] In an earlier rather complete vibrational study[16] of 1,1-dicyclopropylethene, the authors concluded that there was only one conformer present in both fluid phases at ambient temperature, which was the cis-cis (C_{2v}) conformer. This conclusion was consistent with two earlier studies[17,18] in which only one conformer was observed. In one of these studies[18] it was concluded that the cis-cis (C_{2v}) form was present from the solution dipole moment and molar Kerr constant measurements. The conclusions from the vibrational study[16] were based on Raman depolarization data as well as the comparison between the Raman spectrum of the liquid phase with that of the crystalline solid. For the cis-cis C_{2v} form there should be 14 A$_1$ modes to give rise to polarized Raman lines whereas the gauche-gauche rotamer with C_2 symmetry (Figure 1) has 24 A modes and the gauche-gauche′ form with C_s symmetry has 25 A′ modes, so 24 or 25 polarized Raman lines are expected for the gauche-gauche(±) rotamers. The authors[16] dismissed the possibility of the cis-gauche form on the basis that they expected

---

* Corresponding author. Phone: 01 (816)235-6038. Fax: 01 (816)235-2290. E-mail: durigj@umkc.edu.

[‡] University of Missouri−Kansas City.

[†] Taken in part from the thesis of C. Zheng, which will be submitted to the Department of Chemistry, University of Missouri−Kansas City, Kansas City, MO, in partial fulfillment of the Ph.D. degree.

[§] College of Charleston.

10.1021/jp040609c CCC: $30.25

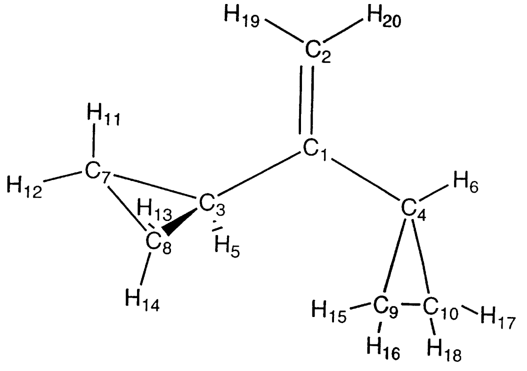

trans-gauche (C_1)

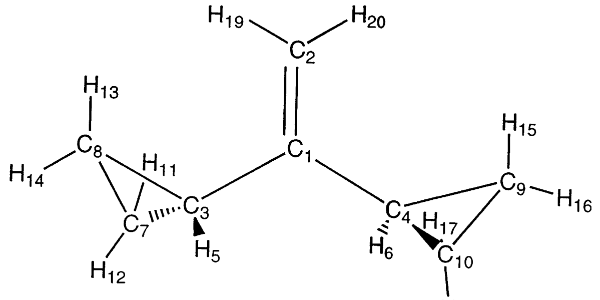

gauche-gauche (C_2)

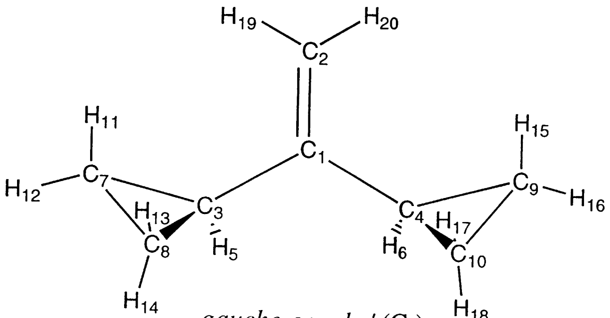

gauche-gauche' (C_s)

Figure 1. Geometric model with atom numbering for the three conformers of 1,1-dicyclopropylethene.

both rings to behave identically, and the trans-trans rotamer was concluded to be sterically impossible based on Dreiding stereomodels. Since 14 of the 25 observed Raman lines were found to be polarized and since little or no coupling was found between the two cyclopropyl rings so that in-phase and out-of-phase motions appeared as single lines, they[16] stated that the 14 polarized Raman lines strongly supported the C_{2v} cis-cis structure. They[16] also concluded that the broad bands in the spectra could be accounted for by the presence of two or more overlapping fundamental vibrations and that no band disappeared upon crystallization of the sample. However, a review of their reported Raman data does not appear to be consistent with this latter observation. For example, there is a very weak, broad Raman line at 1348 cm^{-1} in the spectrum of the liquid that disappears in the spectrum of the solid. Similarly the 800 cm^{-1} shoulder band present in the spectrum of the liquid is not present in the spectrum of the solid. Likewise three additional low-frequency bands at 700 (weak, shoulder), 411 (polarized, shoulder), and 290 (polarized, medium intensity) cm^{-1} in the spectrum of the liquid are not observed in the solid. The last one is of particular interest since it is of medium intensity and it is a low-frequency skeletal bending mode that should be most sensitive to the presence of more than one conformer in the fluid phases. Therefore we believed that the Raman lines which disappeared from the spectrum of the liquid with crystallization were in fact due to a second conformer and we, thus, have launched this investigation on the vibrational spectrum of 1,1-dicyclopropylethene with the expectation of finding more than one conformer in the fluid phases and furthermore to obtain conformational enthalpy difference by studying the temperature dependence of the intensity of fundamentals in xenon solutions.

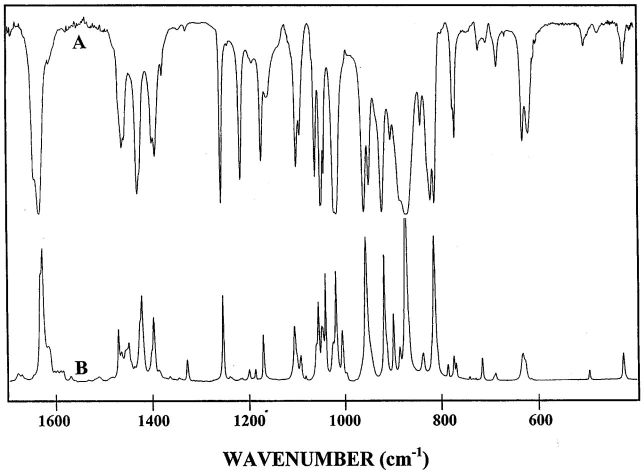

Figure 2. Infrared spectra of 1,1-dicyclopropylethene: (A) gas and (B) annealed solid.

To support the vibrational study we have carried out ab initio calculations with much larger basis sets than the 6-31G(d) used in a rather recent electron diffraction and theoretical investigation[19] of 1,1-dicyclopropylethene. We have carried out calculations with basis sets up to 6-311G(2df,2pd) as well as those with diffuse functions, i.e. 6-311+G(2df,2pd). We found that there can be significant differences in the predicted stabilities of the c-C_3H_5CXO molecules[20−24] with the size of the basis set, particularly with the inclusion of diffuse functions at the MP2 level. We have also carried out density functional theory (DFT) calculations by the B3LYP method with the same basis sets. We have calculated optimized geometries, conformational stabilities, harmonic force fields, infrared intensities, Raman activities, and depolarization ratios. The results of these spectroscopic and theoretical studies are reported herein.

Experimental Section

The 1,1-dicyclopropylethene sample was purchased from Aldrich Chemical Co. with a stated purity of 95%. After several vacuum transfers the sample was found to be 99% pure by NMR. The sample was further purified with a low-pressure, low-temperature fractionation column and the purity of the sample was checked by a comparison of the infrared spectrum to the previously reported one.[16] The purified sample was kept in the dark at low temperature until it was used.

The mid-infrared spectra of the gas (Figure 2A) and solid (Figure 2B) were obtained from 3200 to 220 cm^{-1} on a Perkin-Elmer model 2000 Fourier transform spectrometer equipped with a Ge/CsI beam splitter and a DTGS detector. Atmospheric water vapor was removed from the spectrometer housing by purging with dry nitrogen. The spectrum of the gas was obtained with the sample contained in a 12-cm cell fitted with CsI windows. The spectra of amorphous and crystalline solids were obtained by condensing the sample on a CsI substrate held at the temperature of boiling liquid nitrogen housed in a vacuum cell fitted with CsI windows. The sample was condensed as an

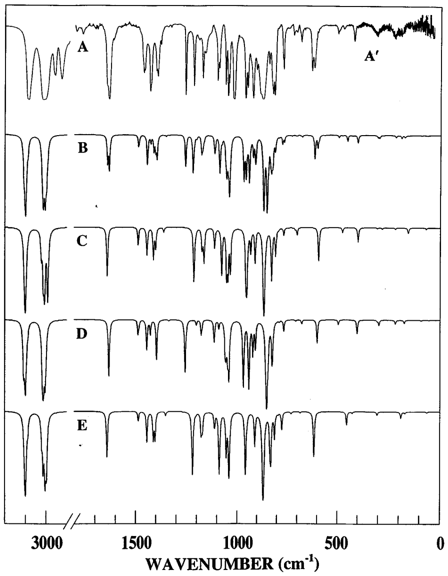

Figure 3. Infrared spectra of 1,1-dicyclopropylethene: (A) xenon solution at −70 °C (A′, gas); (B) calculated spectrum of the mixture of the three conformers at −70 °C with ΔH of 146 and 350 cm^{-1}; (C) calculated spectrum of the gauche-gauche′, C_s conformer; (D) calculated spectrum of the gauche-gauche, C_2 conformer; and (E) calculated spectrum of the trans-gauche conformer.

amorphous solid and repeatedly annealed until no further changes were observed in the spectra. The theoretical resolution used to obtain the spectra of the gas and the solid was 0.5 and 2.0 cm^{-1}, respectively, and usually 128 interferograms were collected and averaged, and the data were transformed using a boxcar truncation function.

The mid-infrared spectra of the sample dissolved in liquefied xenon (Figure 3A) as a function of temperature were recorded on a Bruker model IFS 66 Fourier transform spectrometer equipped with a Globar source, a Ge/KBr beam splitter, and a DTGS detector. In all cases, 100 interferograms were collected at 1.0 cm^{-1} resolution, averaged, and transformed with a boxcar truncation function. For these studies, a specially designed cryostat cell was used. It consists of a copper cell with a path length of 4 cm with wedged silicon windows sealed to the cell with indium gaskets. The copper cell was enclosed in an evacuated chamber fitted with KBr windows. The temperature was maintained with boiling liquid nitrogen and monitored with two Pt thermoresistors. The complete cell was connected to a pressure manifold, which allowed the filling and evacuation of the system. After cooling to the desired temperature, a small amount of the compound was condensed into the cell. Next, the system was pressurized with xenon, which immediately started to condense in the cell, allowing the compound to dissolve.

The far-infrared spectrum (400 to 40 cm^{-1}) of the gas was recorded on the previously described Perkin-Elmer model 2000 spectrometer equipped with a metal grid beam splitter and a DTGS detector. The gas was contained in a cell with a 12 cm path length and equipped with polyethylene windows. Normally 256 scans at a resolution of 0.5 cm^{-1} were used to give a satisfactory signal-to-noise ratio.

The observed wavenumbers for the fundamentals of the trans-gauche (C_1) and gauche-gauche (C_2) conformers are listed in Tables 1 and 2, respectively, along with their predicted values. The predicted wavenumbers for the fundamentals of the least stable gauche-gauche′ (C_s) conformer along with two tentative assignments are listed in Table 3.

Ab Initio Calculations

The LCAO-MO-SCF restricted Hartee-Fock (RHF) calculations were performed with the Gaussian-03 program[25] using Gaussian-type basis functions. The energy minima with respect to nuclear coordinates were obtained by simultaneous relaxation of all geometric parameters consistent with the symmetry restrictions using the gradient method of Pulay.[26] A number of basis sets starting from 6-31G(d) and increasing to 6-311+G-(2df,2pd) were employed at the level of restricted Hartee−Fock and/or Møller−Plesset perturbation theory to the second order (MP2) to obtain energy differences between the three stable conformers (Table 4). Density functional theory calculations were also carried out by the B3LYP method using the same basis sets. From the MP2 calculations with relatively large basis sets beginning with 6-311G(d,p), the trans-gauche rotamers are predicted to be the most stable, ranging in energy from 83 to 141 cm^{-1} lower than the second most stable gauche-gauche (C_2) conformer. The gauche-gauche′ (C_s) rotamer is predicted to be the least stable, on the average by about 350 cm^{-1} with a high value of 403 cm^{-1} and a low of 271 cm^{-1}. The restricted Hartree−Fock calculations predict the gauche-gauche (C_2) form to be the most stable with the other two conformers having similar energies. Similarly the density functional calculations with all the basis sets except the 6-31G(d) predict the gauche-gauche (C_2) rotamer to be the most stable conformer with the trans-gauche form the next most stable conformer (Table 4). The determined structural parameters from some of these calculations are listed in Table 5. These results indicate that the theoretical predictions cannot be relied on to provide the correct conformer stability when the energy differences are about 200 cm^{-1} (2.39 kJ·mol^{-1}) or less. Therefore, one must rely on the experimental determination for establishing the conformational stability order for 1,1-dicyclopropylethene.

To obtain a more complete description of the nuclear motions involved in the vibrational fundamentals of 1,1-dicyclopropylethene, we have carried out normal coordinate analysis. The force fields in Cartesian coordinates were calculated by the Gaussian-03 program[25] at the MP2/6-31G(d) level. The internal coordinates used to calculate the **G** and **B** matrices are listed along with the structural parameters in Table 5 and the numbering is shown in Figure 1. By using the **B** matrix[27] the force field in Cartesian coordinates was converted to a force field in internal coordinates (Table 1S), and the pure ab initio vibrational frequencies were reproduced. Subsequently, scaling factors of 0.88 for the CH stretches and 0.90 for all other modes were used along with the geometric average of scaling factors for interaction force constants to obtain the fixed scaled force field and the resultant wavenumbers. A set of symmetry coordinates was used (Table 2S) to determine the corresponding potential energy distributions (PEDs). A comparison between the observed and calculated wavenumbers of the three stable conformers of 1,1-dicyclopropylethene along with the calculated infrared intensities, Raman activities, depolarization ratios, and PEDs are given in Tables 1, 2, and 3.

To identify the fundamental vibrations for 1,1-dicyclopropylethene from the three possible conformers, the infrared spectra were predicted using fixed scaled frequencies and infrared intensities determined from the Gaussian-03 program[25] from MP2/6-31G(d) calculations. Infrared intensities were calculated based on the dipole moment derivatives with respect to Cartesian coordinates. The derivatives were taken from the ab initio calculations at the MP2/6-31G(d) level and transformed to normal coordinates by $(\partial\mu_u/\partial Q_i) = \sum_j(\partial\mu_u/\partial X_j)L_{ij}$, where Q_i is the ith normal coordinate, X_j is the jth Cartesian displacement

TABLE 1: Observed and Calculated[a] Frequencies (cm^{-1}) for 1,1-Dicyclopropylethene Trans-Gauche (C_1)

vib no.	fundamental	ab initio	fixed scaled[b]	IR int.	Raman act.	dp ratio	IR gas[c]	IR Xe[d]	solid[e]	PED[f]	A[g]	B[g]	C[g]
ν_1	CH_2 antisymmetric stretch	3314	3109	10.7	28.0	0.71	3097	3087	3087	$46S_1$, $41S_{29}$	77	13	10
ν_2	CH_2 antisymmetric stretch	3299	3095	2.0	59.0	0.74	3088	3073	3068	$52S_2$, $35S_{30}$	79	20	1
ν_3	$=CH_2$ symmetric stretch	3213	3014	8.7	19.4	0.48	3020	3005	3005	$47S_3$, $24S_4$, $13S_{31}$	35	46	19
ν_4	CH_2 symmetric stretch	3217	3018	1.1	374.1	0.06	3023	3012	3015	$53S_4$, $23S_3$	88	11	1
ν_5	CH_2 symmetric stretch	3202	3004	8.6	65.2	0.21	3004	2992	2993	$43S_5$, $20S_{32}$, $13S_{31}$, $11S_6$	18	71	11
ν_6	CH stretch	3199	3001	4.3	16.3	0.65	3002	2992	2993	$38S_6$, $32S_{33}$, $13S_4$, $13S_{32}$	18	1	81
ν_7	$C=C$ stretch	1720	1632	12.4	18.8	0.11	1636	1634	1630	$67S_7$, $15S_{10}$	10	90	0
ν_8	CH_2 deformation	1563	1483	0.7	8.9	0.48	1457	1458	1452	$82S_8$, $14S_{12}$	50	49	1
ν_9	CH_2 deformation	1523	1445	4.1	11.7	0.69	1437	1430	1428	$88S_9$, $11S_{35}$	8	28	63
ν_{10}	$=CH_2$ deformation	1504	1427	2.2	21.5	0.23	1400	1400	1400	$65S_{10}$	17	62	21
ν_{11}	CH in-plane bend	1409	1336	0.2	7.6	0.55	1337	1330	1331	$43S_{11}$, $15S_{10}$	60	8	32
ν_{12}	ring breathing	1268	1203	0.4	23.9	0.14	~1189	1198	1202	$40S_{12}$, $22S_{38}$, $11S_{11}$	43	53	4
ν_{13}	CH_2 twist	1242	1178	2.2	3.4	0.73	1177	1174	1173	$45S_{13}$, $44S_{20}$	15	26	59
ν_{14}	CH out-of-plane bend	1174	1114	2.3	1.3	0.69	1097	1101	1108	$63S_{14}$, $29S_{13}$	8	13	79
ν_{15}	CH_2 twist	1150	1091	1.2	4.2	0.75	1097	1094	1095	$25S_{15}$, $16S_{21}$, $15S_{11}$	78	22	0
ν_{16}	CH_2 wag	1113	1056	4.6	0.6	0.45	1059	1051	1049	$58S_{16}$, $25S_{42}$, $13S_{43}$	12	19	69
ν_{17}	CH_2 wag	1104	1047	6.3	1.7	0.31	1027	1023	1021	$52S_{17}$, $17S_{43}$	37	47	16
ν_{18}	ring deformation	971	921	6.1	12.7	0.75	909	906	903	$45S_{18}$, $14S_{45}$	50	22	28
ν_{19}	ring deformation	991	941	18.8	5.8	0.69	925	924	921	$70S_{19}$, $13S_{23}$	2	95	3
ν_{20}	CH_2 rock	869	825	6.3	6.4	0.73	825	823	824	$25S_{20}$, $32S_{18}$, $14S_{14}$, $12S_{13}$	36	36	28
ν_{21}	CH_2 rock	832	789	0.2	1.2	0.59	793	794	790	$61S_{21}$, $16S_{15}$	0	51	49
ν_{22}	$=CH_2$ twist	745	707	0.2	4.3	0.72	727	723	719	$66S_{22}$	10	3	87
ν_{23}	$CC(=C)C$ symmetric stretch	713	677	0.6	7.6	0.15	690	685	692	$28S_{23}$, $15S_{22}$, $13S_{19}$, $11S_{15}$	49	12	39
ν_{24}	ring-C out-of-plane bend	183	174	0.5	0.8	0.67	191		201	$26S_{24}$, $41S_{26}$, $13S_{25}$, $11S_{53}$	3	75	22
ν_{25}	ring-C in-plane bend	321	305	0.2	0.8	0.35	311		337*	$34S_{25}$, $27S_{52}$, $20S_{51}$	64	25	11
ν_{26}	$CC(=C)C$ bend	523	496	0.7	4.3	0.74	504	504	498	$27S_{26}$, $24S_{50}$	31	11	58
ν_{27}	torsion	57	54	0.03	0.3	0.74	65		84*	$94S_{27}$	3	20	77
ν_{28}	$=CH_2$ antisymmetric stretch	3304	3100	19.7	27.5	0.69	3093	3084	3079	$65S_{28}$, $17S_{29}$, $15S_1$	53	25	22
ν_{29}	CH_2 antisymmetric stretch	3309	3104	4.8	61.0	0.74	3096	3087	3087	$31S_{29}$, $33S_{28}$, $26S_1$	30	30	40
ν_{30}	CH_2 antisymmetric stretch	3293	3089	1.3	67.2	0.75		3073	3068	$52S_{30}$, $37S_2$	3	85	12
ν_{31}	CH_2 symmetric stretch	3216	3017	11.8	19.6	0.56	3023	3012	3015	$57S_{31}$, $25S_3$, $14S_5$	60	35	5
ν_{32}	CH_2 symmetric stretch	3211	3012	15.0	45.3	0.54	3014	3005	3005	$55S_{32}$, $33S_5$	14	1	85
ν_{33}	CH stretch	3204	3006	8.3	21.7	0.74	3004	2992	2993	$55S_{33}$, $35S_6$	14	73	13
ν_{34}	CH_2 deformation	1569	1488	2.2	10.2	0.73	1465	1463	1472	$78S_{34}$, $14S_{38}$	18	38	44
ν_{35}	CH_2 deformation	1522	1444	1.4	5.4	0.71	1433	1426	1424	$88S_{35}$	73	24	3
ν_{36}	$CC(=C)C$ antisymmetric stretch	1472	1396	7.6	12.9	0.74	1400	1394	1392	$33S_{36}$, $21S_{37}$, $12S_{34}$	80	18	2
ν_{37}	CH in-plane bend	1324	1256	11.2	14.0	0.36	1260	1257	1256	$51S_{37}$, $19S_{36}$, $12S_{44}$	96	0	4
ν_{38}	ring breathing	1266	1201	0.4	11.8	0.18	1189	1192	1189	$37S_{38}$, $21S_{12}$	15	84	1
ν_{39}	CH_2 twist	1238	1174	0.6	11.3	0.74	1177	1174	1173	$42S_{39}$, $46S_{48}$, $11S_{40}$	75	20	5
ν_{40}	CH out-of-plane bend	1176	1115	1.6	2.3	0.71	1097	1101	1108	$61S_{40}$, $31S_{39}$	79	21	0
ν_{41}	CH_2 twist	1117	1060	5.2	2.9	0.70	1066	1062	1058	$17S_{41}$, $20S_{44}$, $16S_{17}$, $11S_{49}$	77	23	0
ν_{42}	CH_2 wag	1108	1051	1.8	0.5	0.65	1048	1044	1042	$45S_{42}$, $31S_{16}$, $13S_{17}$	68	3	29
ν_{43}	CH_2 wag	1097	1041	13.2	0.7	0.59	1023	1019	1008	$62S_{43}$, $18S_{42}$, $10S_{17}$	72	1	27
ν_{44}	$=CH_2$ wag	1020	968	17.4	8.1	0.74	957	961	959	$29S_{44}$, $37S_{47}$, $15S_{36}$	73	20	7
ν_{45}	ring deformation	957	908	4.7	8.7	0.75	884	886	890	$42S_{45}$	40	6	54
ν_{46}	$=CH_2$ rock	897	851	48.1	1.2	0.74	879	874	876	$77S_{46}$	3	7	90
ν_{47}	ring deformation	890	844	3.6	4.9	0.75	~843	843	842	$27S_{47}$, $21S_{46}$, $14S_{49}$, $12S_{44}$	9	30	61
ν_{48}	CH_2 rock	866	822	4.1	4.1	0.73	818	815	818	$27S_{48}$, $31S_{45}$, $16S_{40}$, $14S_{39}$	51	10	39
ν_{49}	CH_2 rock	808	766	1.7	4.9	0.75	773	773	773	$37S_{49}$, $33S_{41}$	88	8	4
ν_{50}	ring-C in-plane bend	228	216	0.6	2.4	0.73	223		233	$35S_{50}$, $34S_{53}$, $14S_{24}$, $12S_{26}$	13	9	78
ν_{51}	$C=C$ in-plane bend	425	403	2.1	3.7	0.42	426	424	427	$54S_{51}$, $14S_{25}$	88	11	1
ν_{52}	ring-C out-of-plane bend	312	296	0.8	2.0	0.64	311		315	$42S_{52}$, $20S_{50}$, $13S_{24}$, $11S_{25}$	67	1	32
ν_{53}	$C=C$ out-of-plane bend	633	600	3.8	3.3	0.27	635	632	635	$39S_{53}$, $18S_{24}$	14	8	78
ν_{54}	torsion	96	91	0.1	1.2	0.74	93		107	$100S_{54}$	0	99	1

[a] All ab initio frequencies, infrared intensities (km/mol), Raman activities ($Å^4$/u), depolarization ratios, and percentage potential energy distributions are calculated at the MP2(full)/6-31G(d) level with valence electron correlation. [b] Scaled frequencies with scaling factors of 0.88 for CH stretches and 0.90 for all other modes. [c] Infrared spectrum of the gas recorded at 25 °C. [d] Infrared spectrum of the xenon solution recorded at −70 °C. [e] Infrared spectrum of the annealed solid, except those with an asterisk, which are from the Raman spectrum. [f] Symmetry coordinates with PED contribution less than 10% are omitted. [g] Values refer to percentage of A-, B-, and C-type infrared band contour composition.

coordinate, and L_{ij} is the transformation matrix between the Cartesian displacement coordinates and normal coordinates. The infrared intensities were then calculated by $(N\pi)/(3c^2)[(\partial\mu_x/\partial Q_i)^2 + (\partial\mu_y/\partial Q_i)^2 + (\partial\mu_z/\partial Q_i)^2]$. In Figure 3, parts E, D, and C, the simulated infrared spectra of the trans-gauche (C_1), gauche-gauche (C_2), and gauche-gauche′ (C_s) conformers, respectively, are shown. The simulated spectra, calculated at −70 °C, of the mixture of three conformers with the ΔH between the first two conformers obtained from the variable-temperature study in xenon solutions, along with the predicted ΔE for the C_s conformer, is shown in Figure 3B. It should be compared to the experimental spectrum of the xenon solution at −70 °C (Figure 3A). The predicted spectrum is in remarkable resemblance to the experimental spectrum, and the scaled predicted data were proven to be very useful in distinguishing the fundamentals for the three conformers.

Conformational Stability

To obtain reliable enthalpy differences among the conformers, it is important to choose well-defined bands that are relatively

TABLE 2: Observed and Calculated[a] Frequencies (cm^{-1}) for 1,1-dicyclopropylethene Gauche-Gauche (C_2)

block	vib no.	fundamental	ab initio	fixed scaled[b]	IR int.	Raman act.	dp ratio	IR gas[c,h]	IR Xe[d,h]	PED[f]	A[g]	B[g]	C[g]
A	ν_1	CH$_2$ antisymmetric stretch	3305	3101	12.5	42.5	0.60	3097		$94S_1$	–	100	–
A	ν_2	CH$_2$ antisymmetric stretch	3292	3089	2.3	129.2	0.74			$94S_2$	–	100	–
A	ν_3	=CH$_2$ symmetric stretch	3220	3021	4.2	160.8	0.09			$92S_3$	–	100	–
A	ν_4	CH$_2$ symmetric stretch	3212	3013	0.02	165.4	0.04			$70S_4$, $20S_5$	–	100	–
A	ν_5	CH$_2$ symmetric stretch	3202	3004	13.6	117.1	0.12	3005		$74S_5$, $19S_4$	–	100	–
A	ν_6	CH stretch	3196	2998	4.3	22.0	0.24			$91S_6$	–	100	–
A	ν_7	C=C stretch	1730	1641	9.0	11.1	0.07		1645	$69S_7$, $14S_{10}$	–	100	–
A	ν_8	CH$_2$ deformation	1567	1487	0.6	2.6	0.27			$81S_8$, $15S_{12}$	–	100	–
A	ν_9	CH$_2$ deformation	1522	1443	3.0	9.9	0.73			$99S_9$	–	100	–
A	ν_{10}	=CH$_2$ deformation	1488	1412	4.8	20.7	0.21			$76S_{10}$	–	100	–
A	ν_{11}	CH in-plane bend	1424	1351	0.6	10.2	0.21	1348*	1345	$52S_{11}$, $13S_{12}$, $11S_8$	–	100	–
A	ν_{12}	ring breathing	1268	1203	0.1	27.3	0.07			$56S_{12}$, $17S_{11}$, $10S_{15}$	–	100	–
A	ν_{13}	CH$_2$ twist	1238	1174	1.5	15.3	0.71			$42S_{13}$, $45S_{20}$, $11S_{14}$	–	100	–
A	ν_{14}	CH out-of-plane bend	1174	1114	1.0	3.5	0.41			$63S_{14}$, $33S_{13}$	–	100	–
A	ν_{15}	CH$_2$ twist	1144	1085	0.0006	7.2	0.75			$33S_{15}$, $23S_{11}$, $21S_{21}$	–	100	–
A	ν_{16}	CH$_2$ wag	1111	1054	1.1	0.4	0.45			$79S_{16}$, $18S_{17}$	–	100	–
A	ν_{17}	CH$_2$ wag	1099	1042	3.4	0.4	0.69			$72S_{17}$, $20S_{16}$	–	100	–
A	ν_{18}	ring deformation	1000	949	1.0	9.0	0.65			$36S_{18}$, $28S_{19}$	–	100	–
A	ν_{19}	ring deformation	979	929	0.0009	15.2	0.73			$40S_{19}$, $24S_{18}$	–	100	–
A	ν_{20}	CH$_2$ rock	875	830	9.5	6.3	0.71	833	829	$30S_{20}$, $30S_{18}$, $16S_{14}$, $15S_{13}$	–	100	–
A	ν_{21}	CH$_2$ rock	836	793	0.2	1.0	0.47	795	799	$69S_{21}$, $11S_{15}$	–	100	–
A	ν_{22}	=CH$_2$ twist	768	729	0.3	5.8	0.71			$43S_{22}$, $29S_{15}$, $12S_{23}$	–	100	–
A	ν_{23}	CC(=C)C symmetric stretch	720	684	0.1	7.8	0.06	707	700*	$19S_{23}$, $34S_{22}$, $14S_{19}$	–	100	–
A	ν_{24}	ring-C out-of-plane bend	449	426	0.2	3.8	0.65			$37S_{24}$, $27S_{26}$, $12S_{23}$	–	100	–
A	ν_{25}	ring-C in-plane bend	289	274	0.02	2.4	0.26	290*		$85S_{25}$	–	100	–
A	ν_{26}	CC(=C)C bend	179	169	0.2	0.4	0.73	185		$51S_{26}$, $47S_{24}$	–	100	–
A	ν_{27}	torsion	66	63	0.1	0.4	0.71			$99S_{27}$	–	100	–
B	ν_{28}	=CH$_2$ antisymmetric stretch	3310	3105	5.0	66.1	0.75			$82S_{28}$, $16S_{29}$	98	–	2
B	ν_{29}	CH$_2$ antisymmetric stretch	3304	3100	20.4	11.5	0.75	3089		$79S_{29}$, $18S_{28}$	52	–	48
B	ν_{30}	CH$_2$ antisymmetric stretch	3292	3088	0.1	6.4	0.75			$94S_{30}$	86	–	14
B	ν_{31}	CH$_2$ symmetric stretch	3213	3014	13.0	16.2	0.75	3019		$73S_{31}$, $24S_{32}$	89	–	11
B	ν_{32}	CH$_2$ symmetric stretch	3202	3004	8.5	21.0	0.75			$76S_{32}$, $22S_{31}$	0	–	100
B	ν_{33}	CH stretch	3195	2998	11.1	43.9	0.75			$95S_{33}$	20	–	80
B	ν_{34}	CH$_2$ deformation	1566	1486	0.8	12.8	0.75			$78S_{34}$, $16S_{38}$	6	–	94
B	ν_{35}	CH$_2$ deformation	1522	1444	2.4	8.5	0.75			$100S_{35}$	35	–	65
B	ν_{36}	CC(=C)C antisymmetric stretch	1479	1403	4.7	9.7	0.75		1400	$30S_{36}$, $30S_{37}$, $16S_{34}$	100	–	0
B	ν_{37}	CH in-plane bend	1286	1220	15.3	2.3	0.75	1220	1217	$52S_{37}$, $16S_{38}$, $13S_{36}$	94	–	6
B	ν_{38}	ring breathing	1242	1178	3.3	3.8	0.75	1169	1163	$30S_{38}$, $18S_{48}$, $14S_{39}$	70	–	30
B	ν_{39}	CH$_2$ twist	1234	1171	2.5	1.6	0.75			$30S_{39}$, $28S_{48}$, $16S_{38}$	91	–	9
B	ν_{40}	CH out-of-plane bend	1171	1111	1.8	3.3	0.75			$63S_{40}$, $32S_{39}$	1	–	99
B	ν_{41}	CH$_2$ twist	1147	1088	15.1	2.6	0.75	(1097)	(1094)	$31S_{41}$, $18S_{44}$, $18S_{49}$, $10S_{37}$	99	–	1
B	ν_{42}	CH$_2$ wag	1111	1054	7.3	0.1	0.75	1054	1049	$81S_{42}$, $17S_{43}$	27	–	73
B	ν_{43}	CH$_2$ wag	1096	1040	14.8	0.1	0.75	(1023)	(1019)	$77S_{43}$, $17S_{42}$	81	–	19
B	ν_{44}	=CH$_2$ wag	1009	958	15.4	1.7	0.75	947	951	$32S_{44}$, $37S_{47}$, $16S_{36}$	93	–	7
B	ν_{45}	ring deformation	960	910	6.1	18.5	0.75			$71S_{45}$	43	–	57
B	ν_{46}	=CH$_2$ rock	915	868	45.9	0.1	0.75	(884)	(886)	$99S_{46}$	17	–	83
B	ν_{47}	ring deformation	879	834	6.0	0.9	0.75	834	829	$27S_{47}$, $16S_{45}$, $11S_{49}$	6	–	94
B	ν_{48}	CH$_2$ rock	855	811	4.3	0.8	0.75	814		$23S_{48}$, $19S_{49}$, $14S_{40}$, $12S_{39}$, $11S_{47}$	85	–	15
B	ν_{49}	CH$_2$ rock	817	775	2.8	4.4	0.75			$43S_{49}$, $30S_{41}$, $14S_{47}$	86	–	14
B	ν_{50}	ring-C in-plane bend	648	615	8.8	3.1	0.75	619	620	$32S_{50}$, $41S_{53}$, $12S_{41}$	32	–	68
B	ν_{51}	C=C in-plane bend	488	454	2.0	1.5	0.75	476	477	$44S_{51}$, $23S_{52}$	91	–	9
B	ν_{52}	ring-C out-of-plane bend	320	304	0.5	0.3	0.75			$34S_{52}$, $37S_{51}$, $22S_{50}$	74	–	26
B	ν_{53}	C=C out-of-plane bend	200	189	0.9	2.2	0.75			$44S_{53}$, $28S_{52}$, $25S_{50}$	36	–	64
B	ν_{54}	torsion	66	63	0.03	0.4	0.75			$97S_{54}$	58	–	42

[a] All ab initio frequencies, infrared intensities (km/mol), Raman activities (Å^4/u), depolarization ratios, and percentage potential energy distributions are calculated at the MP2/6-31G(d) level with full electron correlation. [b] Scaled frequencies with scaling factors of 0.88 for CH stretches and 0.90 for all other modes. [c] Infrared spectrum of the gas recorded at 25 °C; bands with asterisks are from the Raman spectrum of the liquid. [d] Infrared spectrum of the xenon solution recorded at −70 °C. [f] Symmetry coordinates with PED contribution less than 10% are omitted. [g] Values refer to percentage of A-, B-, and C-type infrared band contour composition; entries with a dash are symmetry forbidden. [h] Observed wavenumbers in parentheses overlap trans-gauche (C_1) bands.

isolated and arise from a single conformer, along with correct assignments. By comparison of the infrared spectrum of the xenon solutions with the infrared spectrum of the annealed solid, several bands can be identified as due to a less stable conformer in the fluid phases. However, it should be noted that the most stable conformer in the solid may not be the most stable one in the fluid states due to packing factors and dipole interactions. The most pronounced band to disappear is the 1217 cm^{-1} band (Figure 2), which is well-separated with appropriate intensity for ΔH determinations. Similarly the pronounced bands at 1163, 951, 829, and 477 cm^{-1} are not present in the spectrum of the solid (Figure 2). The pair at 1257 and 1217 cm^{-1} in the xenon solution are predicted at 1256 (intensity 11.2 km·mol^{-1}) and 1220 (intensity 15.3 km·mol^{-1}) cm^{-1} for the trans-gauche (C_1) and gauche-gauche (C_2) conformers, respectively, which clearly shows that the trans-gauche (C_1) rotamer is the one present in

TABLE 3: Observed and Calculated[a] Frequencies (cm^{-1}) for 1,1-Dicyclopropylethene Gauche-Gauche′ (C_s)

block	vib no.	fundamental	ab initio	fixed scaled[b]	IR int.	Raman act.	dp ratio	IR gas[c]	IR Xe[d,h]	PED[f]	A[g]	B[g]	C[g]
A′	ν_1	CH_2 antisymmetric stretch	3307	3102	20.0	39.6	0.57			$99S_1$	–	29	71
A″	ν_2	CH_2 antisymmetric stretch	3293	3089	0.04	39.0	0.75			$97S_2$	100	–	–
A′	ν_3	$=CH_2$ symmetric stretch	3222	3023	4.4	147.2	0.09			$94S_3$	–	94	6
A′	ν_4	CH_2 symmetric stretch	3212	3013	0.6	210.6	0.02			$87S_4$	–	75	25
A″	ν_5	CH_2 symmetric stretch	3204	3006	1.2	19.3	0.75			$83S_5$, $17S_{31}$	100	–	–
A′	ν_6	CH stretch	3190	2992	21.2	112.9	0.39			$98S_6$	–	6	94
A′	ν_7	C=C stretch	1730	1641	9.9	10.1	0.07			$69S_7$, $15S_{10}$	–	99	1
A′	ν_8	CH_2 deformation	1569	1489	2.8	4.5	0.44			$81S_8$, $15S_{12}$	–	3	97
A″	ν_9	CH_2 deformation	1521	1443	1.4	4.3	0.75			$100S_9$	100	–	–
A′	ν_{10}	$=CH_2$ deformation	1489	1413	5.5	22.3	0.24			$75S_{10}$	–	54	46
A′	ν_{11}	CH in-plane bend	1436	1362	0.7	14.1	0.35			$56S_{11}$, $12S_8$, $11S_{12}$	–	94	6
A′	ν_{12}	Ring breathing	1273	1207	0.4	25.5	0.04			$59S_{12}$, $16S_{11}$	–	77	23
A″	ν_{13}	CH_2 twist	1236	1172	1.1	4.9	0.75			$33S_{13}$, $37S_{20}$	100	–	–
A″	ν_{14}	CH out-of-plane bend	1167	1107	0.008	2.7	0.75			$62S_{14}$, $33S_{13}$	100	–	–
A′	ν_{15}	CH_2 twist	1164	1105	0.1	9.0	0.74			$33S_{15}$, $20S_{21}$, $18S_{11}$	–	43	57
A″	ν_{16}	CH_2 wag	1110	1053	0.8	0.2	0.75			$74S_{16}$, $23S_{43}$	100	–	–
A′	ν_{17}	CH_2 wag	1104	1047	9.6	0.6	0.67			$69S_{17}$, $24S_{42}$	–	3	97
A″	ν_{18}	ring deformation	960	911	6.2	13.5	0.75			$68S_{18}$	100	–	–
A′	ν_{19}	Ring deformation	983	933	3.9	4.1	0.64			$49S_{19}$, $19S_{45}$	–	21	79
A″	ν_{20}	CH_2 rock	852	808	4.6	1.3	0.75			$23S_{20}$, $20S_{49}$, $15S_{14}$, $12S_{47}$, $12S_{13}$	100	–	–
A′	ν_{21}	CH_2 rock	837	794	0.2	0.8	0.16			$73S_{21}$, $10S_{15}$	–	81	19
A″	ν_{22}	$=CH_2$ twist	739	701	1.1	1.0	0.75			$80S_{22}$	100	–	–
A′	ν_{23}	CC(=C)C symmetric stretch	749	710	0.3	8.9	0.36			$25S_{23}$, $35S_{15}$, $11S_{19}$	–	100	0
A″	ν_{24}	ring-C out-of-plane bend	322	306	0.1	0.2	0.75			$42S_{24}$, $35S_{51}$, $18S_{50}$	100	–	–
A′	ν_{25}	ring-C in-plane bend	230	218	0.2	2.4	0.48			$49S_{25}$, $28S_{53}$, $18S_{26}$	–	58	42
A′	ν_{26}	CC(=C)C bend	422	400	2.2	4.9	0.50	415?	418?	$24S_{26}$, $20S_{52}$, $20S_{23}$	–	36	64
A″	ν_{27}	torsion	34	32	0.02	0.1	0.75			$99S_{27}$	100	–	–
A″	ν_{28}	$=CH_2$ antisymmetric stretch	3311	3106	5.0	62.4	0.75			$88S_{28}$, $11S_{29}$	100	–	–
A″	ν_{29}	CH_2 antisymmetric stretch	3304	3100	17.0	9.8	0.75			$87S_{29}$, $12S_{28}$	100	–	–
A′	ν_{30}	CH_2 antisymmetric stretch	3295	3091	0.5	94.8	0.75			$99S_{30}$	–	100	0
A″	ν_{31}	CH_2 symmetric stretch	3212	3013	12.2	22.5	0.75			$81S_{31}$, $17S_5$	100	–	–
A′	ν_{32}	CH_2 symmetric stretch	3206	3007	19.5	55.1	0.26			$91S_{32}$	–	94	6
A″	ν_{33}	CH stretch	3186	2989	0.1	0.9	0.75			$98S_{33}$	100	–	–
A″	ν_{34}	CH_2 deformation	1566	1486	0.02	11.8	0.75			$77S_{34}$, $16S_{38}$	100	–	–
A′	ν_{35}	CH_2 deformation	1524	1446	3.8	12.0	0.71			$98S_{35}$	–	100	0
A″	ν_{36}	CC(=C)C antisymmetric stretch	1478	1402	3.3	3.7	0.75			$31S_{36}$, $28S_{37}$, $16S_{34}$	100	–	–
A″	ν_{37}	CH in-plane bend	1280	1215	12.0	7.0	0.75			$48S_{37}$, $21S_{38}$	100	–	–
A″	ν_{38}	ring breathing	1228	1165	6.1	2.3	0.75			$34S_{38}$, $15S_{44}$, $10S_{36}$	100	–	–
A′	ν_{39}	CH_2 twist	1239	1175	2.9	11.1	0.74			$43S_{39}$, $45S_{48}$, $11S_{40}$	–	81	19
A′	ν_{40}	CH out-of-plane bend	1174	1113	3.3	4.2	0.51			$64S_{40}$, $32S_{39}$	–	76	24
A″	ν_{41}	CH_2 twist	1136	1078	9.4	0.5	0.75			$33S_{41}$, $21S_{49}$, $15S_{37}$, $14S_{44}$	100	–	–
A′	ν_{42}	CH_2 wag	1111	1054	9.5	0.4	0.51			$75S_{42}$, $22S_{17}$	–	49	51
A″	ν_{43}	CH_2 wag	1091	1035	8.6	0.3	0.75			$70S_{43}$, $23S_{16}$	100	–	–
A″	ν_{44}	$=CH_2$ wag	1008	956	12.8	5.4	0.75			$32S_{44}$, $36S_{47}$, $16S_{36}$	100	–	–
A′	ν_{45}	ring deformation	1003	952	14.1	13.7	0.70			$40S_{45}$, $21S_{19}$	–	37	63
A′	ν_{46}	$=CH_2$ rock	912	865	44.7	0.1	0.75	883?	(886)	$98S_{46}$	–	25	75
A″	ν_{47}	ring deformation	883	838	0.02	5.9	0.75			$25S_{47}$, $19S_{18}$	100	–	–
A′	ν_{48}	CH_2 rock	872	827	11.3	6.7	0.73			$30S_{48}$, $29S_{45}$, $18S_{40}$, $16S_{39}$	–	100	0
A″	ν_{49}	CH_2 rock	809	768	1.1	5.0	0.75			$42S_{49}$, $33S_{41}$, $12S_{47}$	100	–	–
A″	ν_{50}	ring-C in-plane bend	297	282	0.2	1.8	0.75			$48S_{50}$, $38S_{24}$	100	–	–
A″	ν_{51}	C=C in-plane bend	503	477	0.7	1.3	0.75			$45S_{51}$, $25S_{50}$	100	–	–
A′	ν_{52}	ring-C out-of-plane bend	164	156	0.8	0.6	0.68			$48S_{52}$, $35S_{26}$, $19S_{53}$	–	92	8
A′	ν_{53}	C=C out-of-plane bend	626	594	5.9	3.4	0.28			$38S_{53}$, $15S_{52}$, $12S_{25}$	–	4	96
A′	ν_{54}	torsion	71	68	0.2	0.5	0.69			$100S_{54}$	–	99	1

[a] All ab initio frequencies, infrared intensities (km/mol), Raman activities (Å^4/u), depolarization ratios, and percentage potential energy distributions are calculated at the MP2/6-31G(d) level with full electron correlation. [b] Scaled frequencies with scaling factors of 0.88 for CH stretches and 0.90 for all other modes. [c] Infrared spectrum of the gas recorded at 25 °C. [d] Infrared spectrum of the xenon solution recorded at −70 °C. [f] Symmetry coordinates with PED contribution less than 10% are omitted. [g] Values refer to percentage of A-, B-, and C-type infrared band contour composition; entries with a dash are symmetry forbidden. [h] Observed wavenumbers in parentheses overlap trans-gauche (C_1) bands.

the crystalline solid. This conclusion is supported by the assignment of other disappearing bands such as the one at 476 cm^{-1} with a predicted frequency of 454 cm^{-1} for the gauche-gauche conformer, whereas the corresponding mode for the trans-gauche form is predicted at 496 cm^{-1}. The only band remaining in this region in the crystalline solid is observed at 498 cm^{-1}, again, clearly showing that the trans-gauche (C_1) form is the one present in the solid. This conclusion is also supported by the earlier reported Raman data where a line was reported at 1348 cm^{-1} in the spectrum of the liquid but not present in the spectrum of the solid. This line is confidently assigned to the gauche-gauche (C_2) conformer where it is predicted at 1351 cm^{-1} with an activity of 10.2 Å^4•u^{-1}; the corresponding mode for the trans-gauche (C_1) form is predicted at 1336 cm^{-1} (activity 7.6 Å^4•u^{-1}) and observed at 1337 cm^{-1} in the infrared spectrum of the gas and at 1330 cm^{-1} in the Raman spectrum of the liquid and this band remains in the Raman spectrum of the solid.

With confident assignments for the 1257 (C_1) and 1217 (C_2) cm^{-1} bands we then used this pair initially to determine which conformer is the most stable rotamer in the xenon solutions.

TABLE 4: Calculated Energies and Energy Differences for the Three Conformers of 1,1-Dicyclopropylethene

method/basis set	trans-gauche	gauche-gauche	ΔE (cm^{-1})	gauche-gauche′	ΔE (cm^{-1})
RHF/6-31G(d)	−309.842281	−309.843461	−259	−309.842177	23
RHF/6-31+G(d)	−309.848349	−309.849599	−274	−309.848357	−2
MP2/6-31G(d)	−310.914974	−310.915014	−9	−310.913696	281
MP2/6-31+G(d)	−310.934053	−310.934278	−49	−310.932816	271
MP2/6-31G(d,p)	−311.014465	−311.014306	35	−311.013076	305
MP2/6-31+G(d,p)	−311.032249	−311.032261	−3	−311.030927	290
MP2/6-311G(d)	−311.134411	−311.134459	−11	−311.133058	297
MP2/6-311+G(d)	−311.141911	−311.141827	18	−311.140428	325
MP2/6-311G(d,p)	−311.226870	−311.226492	83	−311.225306	342
MP2/6-311+G(d,p)	−311.233969	−311.233620	77	−311.232395	345
MP2/6-311G(2d,2p)	−311.312606	−311.311946	145	−311.310772	403
MP2/6-311+G(2d,2p)	−311.317585	−311.316996	129	−311.315887	373
MP2/6-311G(2df,2pd)	−311.440500	−311.439864	140	−311.438742	386
MP2/6-311+G(2df,2pd)	−311.444409	−311.443766	141	−311.442738	367
B3LYP/6-31G(d)	−311.990387	−311.990285	23	−311.989072	289
B3LYP/6-31+G(d)	−312.001784	−312.001957	−38	−312.000786	219
B3LYP/6-311G(d,p)	−312.073410	−312.073757	−76	−312.072622	173
B3LYP/6-311+G(d,p)	−312.075833	−312.076150	−70	−312.075101	160
B3LYP/6-311G(2d,2p)	−312.086188	−312.086484	−65	−312.085360	182
B3LYP/6-311+G(2d,2p)	−312.088547	−312.088798	−55	−312.087794	165
B3LYP/6-311G(2df,2pd)	−312.096463	−312.096723	−57	−312.095634	182
B3LYP/6-311+G(2df,2pd)	−312.098600	−312.098812	−47	−312.097830	169

To obtain the enthalpy difference, spectral data were measured at five-degree intervals between −55 and −100 °C (Figure 4). These sets of intensity data were fit to the van't Hoff equation, $-\ln K = \Delta H/RT - \Delta S/R$, where K is the intensity ratio of C_1/C_2, assuming that ΔH is not a function of temperature in the range of investigation. The value of 106 ± 5 cm^{-1} (Table 6) obtained from this pair is expected to be the lower limit because the 1217 cm^{-1} band clearly has at least one weak band near this frequency in the spectrum of the solid (Figure 2). Since both bands are very symmetric with good intensity along with well-defined baselines, the statistical uncertainty is very small. We then combined the 1217 cm^{-1} band with the 1174 and 961 cm^{-1} bands of the C_1 conformer to obtain additional enthalpy differences. We also used the 951 cm^{-1} band of the gauche-gauche (C_2) conformer to obtain three more enthalpy differences. We tried the pair of bands at 632 and 620 cm^{-1} but the latter one has such a poor signal-to-noise ratio (Figure 4), because of the absorption of the silicon windows, the results were unreliable. All of the meaningful results are listed in Table 6 and there are relatively large variations among the values. Such variations are expected because of the underlying combination and/or overtone bands present in this spectral region, particularly with so many low-frequency bending modes. Nevertheless, by using the average of six band pairs, it is hoped that their effect will cancel out. By using a least-squares fit and the slopes of the van't Hoff plots, an average ΔH value of 146 ± 6 cm^{-1} (1.75 ± 0.07 kJ·mol^{-1}) was obtained with the C_1 conformer the more stable form. The statistical uncertainty is quite low, although there is no doubt on the presence of interference of the measured bands from combinations and overtone bands. Thus, a more reasonable uncertainty is about 20% to provide a more realistic error value. The final value of 146 ± 30 cm^{-1} (1.75 ± 0.36 kJ·mol^{-1}) is obtained for the enthalpy difference between the C_2 rotamer and the more stable C_1 conformer.

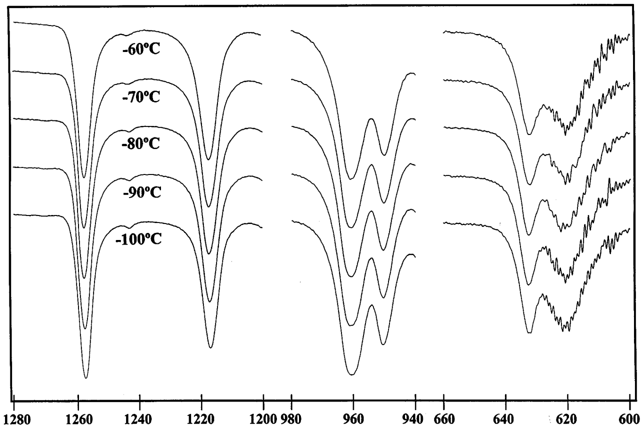

Figure 4. Infrared spectra of 1,1-dicyclopropylethene in xenon solution at different temperatures.

Vibrational Assignment

The vibrational assignment for the more stable C_1 conformer can be made rather straightforwardly based on the ab initio predicted frequencies, the predicted gas-phase band envelopes, and the Raman depolarization ratios. To aid the vibrational assignment we also predicted the Raman spectra for all three of the conformers. The calculated spectra were simulated from ab initio MP2(full)/6-31G(d) scaled frequencies and Raman scattering activities. The Raman scattering cross-sections, $\partial\sigma_j/\partial\Omega$, which are proportional to the Raman intensities, can be calculated from the scattering activities and the predicted frequencies for each normal mode.[28−31] To obtain the polarized Raman scattering cross sections, the polarizabilities are incorporated into S_j by multiplying S_j by $(1 - \rho_j)/(1 + \rho_j)$, where ρ_j is the depolarization ratio of the jth normal mode. The Raman scattering cross sections and calculated scaled frequencies were used together with a Lorentzian function to obtain the calculated spectrum. The predicted Raman spectra of the trans-gauche (C_1), gauche-gauche (C_2), and gauche-gauche′ (C_s) conformers are shown in Figure 5, parts E, D, and C, respectively. The spectrum of the mixture of the three conformers utilizing the predicted ΔE for the C_s form and the experimental ΔH value for the C_2 form, calculated at 25°C, is shown in Figure 5B; the experimental Raman spectrum of the liquid at ambient temperature is shown in Figure 5A. The agreement between the predicted and observed spectra is reasonably good but not nearly as good as the agreement of the simulated infrared spectrum due to the significantly stronger intermolecular interaction in the liquid phase. Nevertheless, these spectra were of considerable aid in making the vibrational assignment for the two most abundant conformers.

TABLE 5: Structural Parameters (Å and Degree), Rotational Constants (MHz), and Dipole Moments (D) for the Three Stable Rotamers of 1,1-Dicyclopropylethene

structural parameters	internal coord	MP2/6-311+G(d,p)			electron diffraction[a]			adjusted r_0		
		tg (C_1)	*gg* (C_2)	*gg′* (C_s)	r_a *tg* (C_1)	r_a *gg* (C_2)	r_a *gg* (C_2)	*tg* (C_1)	*gg* (C_2)	*gg′* (C_s)
$r(C_1{=}C_2)$	R_1	1.348	1.345	1.345	1.331	1.3271	1.3205(30)	1.336	1.336	1.336
$r(C_1C_3)$	R_2	1.490	1.489	1.490	1.496	1.4960	1.4930(26)	1.490	1.489	1.490
$r(C_1C_4)$	R_3	1.486	1.489	1.490	1.494	1.4960	1.4930(26)	1.486	1.489	1.490
$r(C_3C_7)$	R_4	1.507	1.505	1.505	1.511	1.5120	1.4970(11)	1.508	1.506	1.506
$r(C_3C_8)$	R_5	1.518	1.517	1.516	1.511	1.5120	1.4970(11)	1.519	1.518	1.517
$r(C_7C_8)$	R_6	1.508	1.510	1.511	1.511	1.512	1.497(1)	1.511	1.513	1.514
$r(C_4C_9)$	R_7	1.516	1.505	1.505	1.511	1.5120	1.4970(11)	1.517	1.506	1.506
$r(C_4C_{10})$	R_8	1.517	1.517	1.516	1.511	1.5120	1.4970(11)	1.518	1.518	1.517
$r(C_9C_{10})$	R_9	1.505	1.510	1.511	1.511	1.512	1.497(1)	1.508	1.513	1.514
$r(C_2H_{19})$	r_1	1.084	1.085	1.085				1.084	1.085	1.085
$r(C_2H_{20})$	r_2	1.086	1.085	1.085				1.086	1.085	1.085
$r(C_3H_5)$	r_3	1.087	1.088	1.088		1.0931	1.0598(12)	1.087	1.088	1.088
$r(C_4H_6)$	r_4	1.087	1.088	1.088		1.0931	1.0598(12)	1.087	1.088	1.088
$r(C_7H_{11})$	r_5	1.083	1.083	1.083		1.0931	1.0598(12)	1.083	1.083	1.083
$r(C_8H_{13})$	r_7	1.085	1.084	1.084		1.0931	1.0598(12)	1.085	1.084	1.084
$r(C_7H_{12})$	r_6	1.084	1.084	1.084		1.0931	1.0598(12)	1.084	1.084	1.084
$r(C_8H_{14})$	r_8	1.084	1.084	1.084		1.0931	1.0598(12)	1.084	1.084	1.084
$r(C_9H_{15})$	r_9	1.083	1.083	1.083		1.0931	1.0598(12)	1.083	1.083	1.083
$r(C_{10}H_{17})$	r_{11}	1.083	1.085	1.084		1.0931	1.0598(12)	1.083	1.085	1.084
$r(C_9H_{16})$	r_{10}	1.084	1.084	1.084		1.0931	1.0598(12)	1.084	1.084	1.084
$r(C_{10}H_{18})$	r_{12}	1.084	1.084	1.084		1.0931	1.0598(12)	1.084	1.084	1.084
$\angle C_3C_1C_4$	λ	117.6	113.7	113.8				117.6	113.7	113.8
$\angle C_3C_1C_2$	κ_1	122.3	123.1	123.1			122.95(33)	122.3	123.1	123.1
$\angle C_4C_1C_2$	κ_2	120.1	123.1	123.1			122.95(33)	120.1	123.1	123.1
$\angle C_1C_3C_7$	μ_1	121.9	122.4	122.8				121.9	122.4	122.8
$\angle C_1C_3C_8$	μ_2	119.4	118.8	119.6				119.4	118.8	119.6
$\angle C_1C_4C_9$	ν_1	121.7	122.4	122.8				121.7	122.4	122.8
$\angle C_1C_4C_{10}$	ν_2	121.4	118.8	119.6				121.4	118.8	119.6
$\angle C_7C_3C_8$		59.8	59.6	60.0	60.0	60.0	60.0	59.8	59.6	60.0
$\angle C_3C_7C_8$		60.5	60.0	60.4	60.0	60.0	60.0	60.5	60.0	60.4
$\angle C_3C_8C_7$		59.7	60.4	59.6	60.0	60.0	60.0	59.7	60.4	59.6
$\angle C_9C_4C_{10}$		59.5	60.0	59.6	60.0	60.0	60.0	59.5	60.0	59.6
$\angle C_4C_9C_{10}$		60.3	60.4	60.4	60.0	60.0	60.0	60.3	60.4	60.4
$\angle C_4C_{10}C_9$		60.2	59.6	60.0	60.0	60.0	60.0	60.2	59.6	60.0
$\angle C_1C_2H_{19}$	σ_1	121.7	121.2	121.3			121.57	121.7	121.2	121.3
$\angle C_1C_2H_{20}$	σ_2	120.8	121.2	121.3			121.57	120.8	121.2	121.3
$\angle H_{19}C_2H_{20}$	ϕ	117.6	117.6	117.5				117.6	117.6	117.5
$\angle C_1C_3H_5$	ζ_1	115.2	114.3	114.1			114.11	115.2	114.3	114.1
$\angle C_7C_3H_5$	η_1	114.8	116.0	115.5				114.8	116.0	115.5
$\angle C_8C_3H_5$	η_2	114.5	114.5	114.3				114.5	114.5	114.3
$\angle C_1C_4H_6$	ζ_2	114.0	114.3	114.1			114.11	114.0	114.3	114.1
$\angle C_9C_4H_6$	θ_1	115.1	114.5	115.5				115.1	114.5	115.5
$\angle C_{10}C_4H_6$	θ_2	114.6	116.0	114.3				114.6	116.0	114.3
$\angle C_3C_7H_{11}$	α_1	118.1	117.9	118.0				118.1	117.9	118.0
$\angle C_3C_7H_{12}$	α_2	117.4	117.7	117.6				117.4	117.7	117.6
$\angle C_8C_7H_{11}$	α_3	117.1	117.0	117.0				117.1	117.0	117.0
$\angle C_8C_7H_{12}$	α_4	118.0	118.0	118.0				118.0	118.0	118.0
$\angle C_3C_8H_{13}$	β_1	116.2	116.5	116.5				116.2	116.5	116.5
$\angle C_3C_8H_{14}$	β_2	118.3	118.2	118.3				118.3	118.2	118.3
$\angle C_7C_8H_{13}$	β_3	116.9	116.8	116.9				116.9	116.8	116.9
$\angle C_7C_8H_{14}$	β_4	118.5	118.5	118.6				118.5	118.5	118.6
$\angle H_{11}C_7H_{12}$	ϵ_1	115.1	115.1	115.0			114.53	115.1	115.1	115.0
$\angle H_{13}C_8H_{14}$	ϵ_2	115.7	115.6	115.6			114.53	115.7	115.6	115.6
$\angle C_4C_9H_{15}$	γ_1	117.2	116.5	118.0				117.2	116.5	118.0
$\angle C_4C_9H_{16}$	γ_2	117.2	118.5	117.6				117.2	118.2	117.6
$\angle C_{10}C_9H_{15}$	γ_3	117.3	116.8	117.0				117.3	116.8	117.0
$\angle C_{10}C_9H_{16}$	γ_4	118.1	117.7	118.0				118.1	118.5	118.0
$\angle C_4C_{10}H_{17}$	δ_1	117.8	117.9	116.5				117.8	117.9	116.5
$\angle C_4C_{10}H_{18}$	δ_2	117.0	118.2	118.3				117.0	117.7	118.3
$\angle C_9C_{10}H_{17}$	δ_3	117.6	117.0	116.9				117.6	117.0	116.9
$\angle C_9C_{10}H_{18}$	δ_4	118.3	118.0	118.6				118.3	118.0	118.6
$\angle H_{15}C_9H_{16}$	ϵ_3	115.6	115.6	115.0			114.53	115.6	115.6	115.0
$\angle H_{17}C_{10}H_{18}$	ϵ_4	115.0	115.1	115.6			114.53	115.0	115.1	115.6
$\tau C_7C_3C_1C_2$	τ_1	−21.7	−23.9	−20.1				−21.7	−23.9	−20.1
$\tau C_8C_3C_1C_2$	τ_1	−92.5	−94.7	−91.5				−92.5	−94.7	−91.5
$\tau C_9C_4C_1C_2$	τ_2	147.4	−94.7	20.1				147.4	−94.7	20.1
$\tau C_{10}C_4C_1C_2$	τ_2	−141.5	−23.9	91.5				−141.5	−23.9	91.5
$\tau C_7C_3C_1H_5$		−147.0	−149.0	−148.0				−147.0	−149.0	−148.0
$\tau C_8C_3C_1H_5$		142.2	140.2	140.5				142.2	140.2	140.5
$\tau C_9C_4C_1H_6$		145.1	140.2	148.0				145.1	140.2	148.0

TABLE 5: (Continued)

structural parameters	internal coord	MP2/6-311+G(d,p)			electron diffraction[a]			adjusted r_0		
		tg (C_1)	*gg* (C_2)	*gg′* (C_s)	r_a *tg* (C_1)	r_a *gg* (C_2)	r_a *gg* (C_2)	*tg* (C_1)	*gg* (C_2)	*gg′* (C_s)
$\tau C_{10}C_4C_1H_6$		−143.7	−149.0	−140.5				−143.7	−149.0	−140.5
$\tau H_{11}C_7C_3C_1$		−1.0	−0.1	−1.0				−1.0	−0.1	−1.0
$\tau H_{13}C_8C_3C_1$		4.8	5.9	6.0				4.8	5.9	6.0
$\tau H_{12}C_7C_3C_1$		143.9	144.9	144.0				143.9	144.9	144.0
$\tau H_{14}C_8C_3C_1$		−139.8	−138.8	−138.7				−139.8	−138.8	−138.7
$\tau H_{15}C_9C_4C_1$		2.8	5.9	1.0				2.8	5.9	1.0
$\tau H_{17}C_{10}C_4C_1$		−3.2	−0.1	−6.0				−3.2	−0.1	−6.0
$\tau H_{16}C_9C_4C_1$		−141.2	−138.8	−144.0				−141.2	−138.8	−144.0
$\tau H_{18}C_{10}C_4C_1$		140.5	144.9	138.7				140.5	144.9	138.7
A		3329.2	4357.5	4048.7				3341.6	4374.0	4062.3
B		1601.1	1285.7	1397.2				1600.7	1285.0	1396.7
C		1255.1	1123.2	1165.2				1256.7	1124.0	1165.8
$\lvert\mu_a\rvert$		0.188								
$\lvert\mu_b\rvert$		0.616	0.557	0.554						
$\lvert\mu_c\rvert$		0.069		0.219						
$\lvert\mu_t\rvert$		0.648	0.557	0.596						

[a] Reference 19. [b] Calculated from ref 19 results.

TABLE 6: Temperature-Dependent Intensity Ratios for the Trans-Gauche (C_1) and Gauche-Gauche (C_2) Conformers of 1,1-Dicyclopropylethene Dissolved in Liquid Xenon

T (°C)	1000/*T* (K^{-1})	I_{1257tg}/I_{1217gg}	I_{1174tg}/I_{1217gg}	I_{961tg}/I_{1217gg}	I_{1257tg}/I_{951gg}	I_{1174tg}/I_{951gg}	I_{961tg}/I_{951gg}
−55.0	4.5840	0.98473	0.57031	4.91597	0.50239	0.67921	2.50806
−60.0	4.6915	0.99214	0.59078	5.09798	0.50773	0.70482	2.60893
−65.0	4.8042	0.99260	0.61358	5.20813	0.51259	0.72554	2.68756
−70.0	4.9225	1.01785	0.63636	5.37213	0.52275	0.74834	2.75901
−75.0	5.0467	1.03760	0.66265	5.65126	0.52992	0.78055	2.88621
−80.0	5.1773	1.07395	0.68859	5.91121	0.53744	0.80140	2.95814
−85.0	5.3149	1.08426	0.71052	6.05760	0.54395	0.82576	3.03899
−90.0	5.4600	1.11548	0.73873	6.32796	0.55866	0.85980	3.16921
−95.0	5.6132	1.12893	0.76857	6.55676	0.56611	0.88918	3.28796
−100.0	5.7753	1.17388	0.80404	6.99177	0.57869	0.91953	3.44679
Δ*H* (cm^{-1})	individual pair	106 ± 5	166 ± 4	202 ± 5	83 ± 2	143 ± 1	179 ± 4
Δ*H* (cm^{-1})	statistical av			146 ± 6			

For the most stable trans-gauche conformer, we have listed the frequencies of the observed fundamentals in the gaseous, xenon solution, and solid phases (Table 1). In many cases the frequencies for the gas had to be estimated from the spectra of the xenon solutions since the vibrations for the two cyclopropyl rings are overlapped with additional contributions from the modes of the C_2 conformer (Figure 6). Additionally most of the fundamentals in both infrared and Raman spectra of crystalline solid are doublets with a few of them exhibiting some shifts which is an indication that there are two molecules per primitive cell. Only a few bands involve assignments that are difficult, or questionable, or differ significantly from those previously reported.[16] Therefore only these latter vibrations will be discussed.

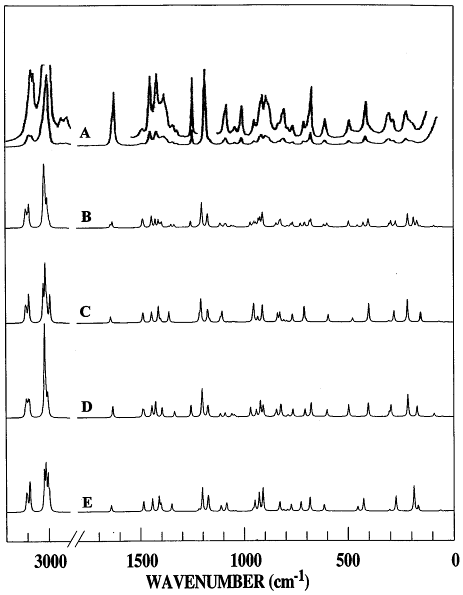

Figure 5. Raman spectra of 1,1-dicyclopropylethene: (A) liquid at 25 °C; (B) calculated spectrum of the mixture of three conformers with Δ*H* of 146 and 350 cm^{-1}; (C) calculated spectrum of the gauche-gauche′, C_s conformer; (D) calculated spectrum of the gauche-gauche, C_2 conformer; and (E) calculated spectrum of the trans-gauche conformer.

For many monosubstituted three-membered-ring molecules, the C−H stretch on the carbon with the substituent is between

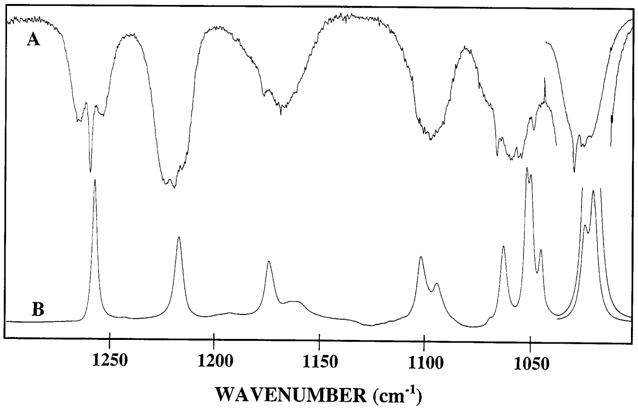

Figure 6. Infrared spectra in the region of 1000 to 1300 cm^{-1} of 1,1-dicyclopropylethene: (A) gas and (B) xenon solution at −70 °C.

the CH_2 antisymmetric and symmetric stretches; this is the order adopted in the earlier assignment, but the ab initio calculations predict this mode to be essentially accidentally degenerate with the CH_2 symmetric stretch. In terms of the bending modes, with a scaling factor of 0.9 the carbon−hydrogen deformations are predicted too high, but there is little question concerning these assignments based on the infrared spectra of the xenon solution. The predicted frequencies for two of the other $=CH_2$ bends ($=CH_2$ twist and $=CH_2$ rock) are observed 20 cm^{-1} or more higher than the predicted values. The only place where there is some question concerning the order of a conformer pair is the two bands at 632 and 620 cm^{-1}, where the band in the infrared spectrum of the solid appears to originate from the 620 cm^{-1} band in the xenon solution. However, since we have found that the predicted frequency order for modes of conformers of hydrocarbons is consistent with the observed order, we have assigned the lower frequency band of this pair to the C_2 conformer.

Once the fundamentals have been assigned for the C_1 form, there is little trouble in assigning the gauche-gauche (C_2) bands which disappear from the Raman spectrum of the liquid or from the infrared spectrum of the xenon solution when they are compared to the corresponding spectra of the solid. These assignments are listed in Table 2 along with the predicted values. Several weak bands could be assigned as fundamentals of the C_2 conformer but it is possible that several of these could be combination and/or overtone bands. Also many of the fundamentals for the C_2 form are nearly accidentally degenerate with similar modes of the more stable C_1 form.

A diligent search for evidence of the third conformer results in only two possibilities. The C=C in-plane bend fundamental is reasonably well separated for the three conformers. The one for the C_1 conformer is predicted at 403 cm^{-1} and observed at 426 cm^{-1}. The corresponding C_2 band is predicted at 454 cm^{-1} and observed at 476 cm^{-1}. There is a Q-branch at 415 cm^{-1} that could be due to the gauche-gauche′ (C_s) form (predicted at 400 cm^{-1}). Another possibility of identifying the C_s conformer lies with the strongest infrared band in the entire spectrum, the $=CH_2$ rock. The band at 883 cm^{-1} could be due to the C_s rotamer but it is obscured by the much more intense fundamental of the most stable conformer at 879 cm^{-1}. Thus only very limited experimental evidence could be suggested for the presence of the third conformer.

Discussion

The MP2/6-31G(d) ab initio calculations with the two scaling factors predict the observed fundamentals for the C_1 conformer to within an average error of 10 cm^{-1}, which represents only a 0.75% error. This relatively small basis set with only two scaling factors predicts both the frequencies and the relative intensities of the infrared spectrum remarkably well and there is no distinct need to use multiple scaling factors for the spectroscopic predictions.

There is extensive mixing of the modes for the C_1 conformer even for the heavy atom modes. For example, the in-plane ring breathing mode has 40% S_{12} and 22% S_{38} for the fundamental at 1198 cm^{-1}, whereas for the out-of-plane motion at 1192 cm^{-1} the contributions are 37% S_{38} and 21% S_{12}. The CH_2 twists, CH_2 rocks, and the heavy atom bends involve extensive mixing with significant contributions from four or more symmetry coordinates (Table 1). Therefore, the descriptions for several of these modes are rather arbitrary, but for many of the other ones the major contribution is greater than 50% and the approximate descriptions provide a reasonable view of the nuclear motions. Of course the mixing is significantly reduced for the C_2 and C_s conformers because of the symmetry (Tables 2 and 3).

Since the structural parameters for the conformers differ very little, the corresponding force constants are nearly the same for all three conformers; in addition, the mixing for the low-frequency skeletal bends is also similar among the conformers. Therefore, there is little difference in the frequencies of the corresponding modes for the three conformers. The major differences in going from the trans-gauche (C_1) to gauche-gauche (C_2) form are for the force constants of the $\angle C_1C_2C_3$, $\angle C_1C_4C_{10}$, and $\angle C_3C_1C_4$ bends which decrease by 11%, 16%, and 23%, respectively. On the other hand, the $\angle C_1C_3C_7$ bend force constant increases by 21% whereas that for the $\angle C_1C_3C_8$ bend increases by 17%. These changes reflect the significant change in angles when the trans cyclopropyl ring rotates to the gauche position. There are some significant changes (11%) in the force constants for the $\angle C_1C_4H_6$ and $\angle C_8C_3H_5$ bends, but for most of the other force constants the changes are less than 2% for the corresponding ones between the C_1 and C_2 conformers.

Of major interest in this research is the conformational stability wherein the initial vibrational investigation it was concluded that only one conformer was present in the fluid phases and it was the cis-cis (C_{2v}) form that was consistent with the predicted stability from MINDO/3 calculations.[32] However, from an initial electron diffraction investigation,[33] it was not possible to identify the conformation but an ab initio calculation with the 4-31G basis set[34] predicted the gauche-gauche (C_2) form as the most stable conformer. This conclusion was also reached in a more recent electron diffraction study[19] where the conformer stability was determined to be 59% gauche (47% gauche-gauche, C_2, and 11% gauche-gauche′, C_s) and 41% trans-gauche (C_1). Our results are in contrast to all of these earlier results where clearly the trans-gauche (C_1) form is the only one remaining in the annealed solid, and this form is more stable in liquid xenon where the determined ΔH value is expected to be near the value in the gas.[35−39] The ΔH of 146 ± 30 cm^{-1} is sufficiently large that the small association with xenon can have little differential effect on the two most abundant conformers since they have similar values of dipole moments. Therefore we believe the electron diffraction results are in error and probably resulted from heavy reliance on the low-to-medium level ab initio predicted stability where the calculations were performed with very small basis sets, apparently with frozen core treatment. We carried out similar calculations with the same basis set with (full) electron correlation and the C_2 conformer is predicted more stable by only 9 cm^{-1} (Table 4) rather than the value of 73 cm^{-1} that was reported[19] earlier. On the low end of our calculations, the Hartree−Fock method predicted the C_2 form to be more stable by more than 250 cm^{-1}! Also for a molecule as large as 1,1-dicyclopropylethene, there are so many structural parameters that the theoretical diffraction curves for the C_1, C_2, and C_s forms become very similar, so obtaining the relative amounts of the three conformers by means of numerous band deconvolutions must be a daunting task, which is why the earlier electron diffraction study[19] did not give definitive curve fitting results.

To support the ΔH value obtained from the variable-temperature infrared spectra, we also calculated the enthalpy difference between the C_1 and C_2 conformers utilizing a single temperature and the predicted infrared intensities from the MP2-(full)/6-31G(d) ab initio calculations. Then enthalpy difference is determined by the equation $\Delta H = -kT \ln[(g_{C_1}\cdot I_{C_2}\cdot \epsilon_{C_1})/(g_{C_2}\cdot$

$I_{C_1}\cdot\epsilon_{C_2})]$, where g is the degeneracy of each conformer, I is the observed infrared intensity, and ϵ is the ab initio predicted infrared intensity. Given statistical weights $g_{C_1}/g_{C_2} = 2$, the equation is reduced to $\Delta H = -kT \ln[2(I_{C_2}\cdot\epsilon_{C_1})/(I_{C_1}\cdot\epsilon_{C_2})]$. By utilizing the peak heights from four conformer pairs at the lowest temperature where the bands are the sharpest, we obtained a value of 124 cm^{-1}, which is well within the experimental value of 146 ± 30 cm^{-1}. We have used this method for some organophosphorus molecules where as many as 12 conformer pairs were utilized and the results were always within the totally experimentally determined values from the variable-temperature van't Hoff plot, so long as certain predicted intensities which have been known to involve large systematic errors from MP2 calculations were dropped. However, it should be noted that this method works only if the predicted intensities are reasonable and many conformer pairs are available.

The failure to recognize the presence of conformers in the earlier vibrational study[16] was partially due to the fact that most of the fundamentals for the three conformers have nearly the same frequencies. Only five bands had significantly different frequencies from the most stable conformer and they were obviously missing in the spectrum of the solid. Presumably these earlier investigators did not consider the disappearance of these five bands sufficient to postulate the presence of a second conformer in the liquid. By using the ΔH of 146 cm^{-1} for the C_2 form and the predicted average of 350 cm^{-1} for the C_s form, estimated conformation abundance was obtained at ambient temperature with 75% C_1, 19% C_2, and 6% C_s. As suggested earlier,[19] it is interesting to compare the relative conformer stability of the 1,1-dicyclopropylethene to that of the corresponding monosubstituted molecule, i.e., vinylcyclopropane, which exists mainly as the trans conformer (77% trans, 23% gauche).[40] If the disubstituted molecule is considered to be constructed from vinylcyclopropane with an additional cyclopropyl group, and if the trans-trans conformer of the disubstituted molecule is considered unacceptable, a mixture of 77% of the trans-gauche and 23% of the gauche-gauche form would be anticipated. This assumes that the two cyclopropyl groups have negligible interaction. These are nearly the values we obtained in this study, which indicates very little steric repulsion between the trans and gauche cyclopropyl groups.

The stable conformers of 1,1-dicyclopropylethene are in contrast to those of dicyclopropyl ketone where the most stable conformer is the cis-cis (C_{2v}) conformer (C=O bond over the two three-membered ring). The minor conformer (13 ± 2% at ambient temperature) is the cis-trans (C_s) form where the C=O bond is eclipsing the hydrogen atom on one of the rings. The enthalpy difference between these two conformers has been determined to be 530 ± 27 cm^{-1} (6.34 ± 0.32 kJ·mol^{-1}) and the theoretical predictions are consistent with these experimental results. These significantly different conformational stabilities between these two isoelectronic molecules clearly show the steric effect of the hydrogen atoms on the ethene part of 1,1-dicyclopropylethene where a cis form is not even present.

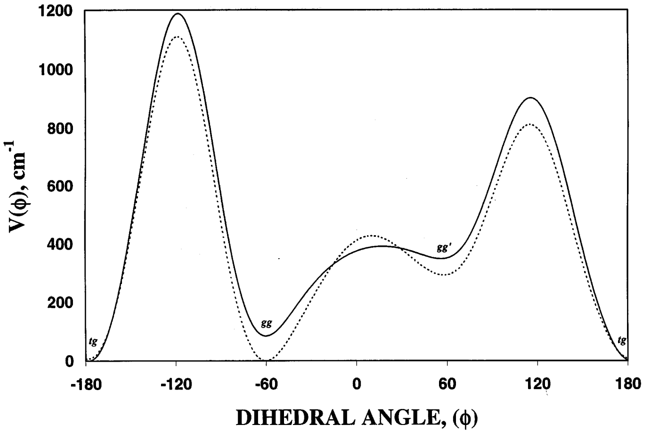

Figure 7. Asymmetric torsional potential function for 1,1-dicyclopropylethene. The solid curve corresponds to the potential function calculated at the MP2(full)/6-311G(d,p) level and the dotted curve corresponds to the one calculated at the MP2(full)/6-31G(d) level. A torsional dihedral angle of ca. 180° corresponds to the most stable trans-gauche conformer, ca. −60° the second most stable gauche-gauche conformer, and ca. 60° the least stable gauche-gauche′ conformer.

TABLE 7: Calculated Potential Barriers and Fourier Potential Coefficients of 1,1-Dicyclopropylethene

	MP2(Full)/ 6-31G(d)	MP2(Full)/ 6-311G(d,p)
coeff (cm^{-1})		
V_1	186	207
V_2	349	447
V_3	−672	−671
V_4	106	140
V_5	84	92
V_6	−38	−36
V'_1	34	21
V'_2	251	217
V'_3	2	6
V'_4	−98	−107
V'_5	44	37
potential barriers (cm^{-1})		
$tg \rightarrow gg$	1103	1188
$tg \rightarrow gg'$	805	902
$gg \rightarrow tg$	1110	1104
$gg \rightarrow gg'$	427	307
$gg' \rightarrow tg$	519	554
$gg' \rightarrow gg$	135	43

The asymmetric cyclopropyl torsional potential has been predicted from ab initio calculations. Beginning at the minimum for the most stable trans-gauche conformer, a potential function was determined by keeping one cyclopropyl group in the gauche position with respect to the double bond (dihedral ~60°) while rotating the other cyclopropyl group (starting from trans position, dihedral ~180°) at 30° intervals throughout a 360° cycle. The energies were calculated with full optimization of all structural parameters, except for the varying dihedral angle at increments of 30°, at each point from MP2(full)/6-31G(d) and MP2(full)/6-311G(d,p) calculations. All three stable conformers appear as minima on the plot, i.e., dihedral angles ~180°, ~ −60°, and ~60° correspond to the trans-gauche, gauche-gauche, and gauche-gauche′ conformers, respectively. Two of the three maxima correspond to alternative C_2 and C_s symmetry forms where the gauche dihedral angles are ~120° rather than ~60° in the stable conformers, the cis-gauche orientation (dihedral ~0°) is also predicted to be a maximum, although it is the lowest energy transition state. The calculated potential functions are shown in Figure 7. Utilizing a Fourier cosine and sine series to represent the asymmetric potential function with the form $V(\phi) = \sum_{i=1}^{6}(V_i/2)(1 - \cos i\phi) + \sum_{i=1}^{5}(V_i'/2)(\sin i\phi)$, the potential constants for the first six cosine terms and the first five sine terms were obtained. The potential constants, calculated at MP2(full)6-31G(d) and MP2(full)6-311G(d,p) levels, are listed in Table 7. Of particular interest is the extremely small predicted value for the gauche-gauche′ to gauche-gauche barrier of only 43 cm^{-1} from the MP2(full)6-311G(d,p) calculation, which is the lowest MP2 level to yield correct conformational stability. For the gauche-gauche′ form, the A′ torsional fundamental, which is predicted to be 10 times more intense than the corresponding A″ mode, is predicted at 68 cm^{-1}. This value plus the zero-point energy is more than two times larger than the MP2(full)6-311G(d,p) predicted potential barrier, which suggests the gauche-gauche′ well may be too shallow to withhold the vibrational transition between the ground and the virtual first excited state. This, along with the large energy difference between the gauche-gauche′ form and the most stable trans-gauche conformer, may account for the lack of spectroscopic evidence for the presence of the gauche-gauche′ form.

The predicted structural parameters for the trans and gauche cyclopropyl groups are remarkably similar. For example, the C_1-C_3 (gauche) and C_1-C_4 (trans) distances only differ by 0.004 Å between the two groups (Table 5). Similarly the opposite C_7-C_8 (gauche) and C_9-C_{10} (trans) distances in the rings differ by only 0.003 Å with the one in the gauche position having the longer distance, the same as what was found for the attached carbon−carbon bond in similar molecules. The $\angle C_4C_1C_2$ is predicted to be 3° smaller for the trans cyclopropyl group compared to the corresponding angle for the gauche one whereas the $\angle C_3C_1C_4$ opens about 4° for the C_1 conformer compared to the similar angles for the other two conformers.

We have found for several monosubstituted cyclopropyl molecules[15,20,41] the ab initio MP2(full)/6-311+G(d,p) predicted heavy atom parameters need to be adjusted by only 0.002 to 0.003 Å, and the adjusted of carbon−hydrogen distances are no more than 0.002 Å of the reported values, to fit the reported microwave rotational constants. Therefore it is believed that the adjusted r_0 structural parameters listed in Table 5 are more accurate than those obtained from the electron diffraction study. If one takes the average of the three different carbon−carbon distances for the trans cyclopropyl group, one obtains the average 1.512 Å, which is the same value as reported from the recent electron diffraction study[19] and is only 0.001 Å longer than the average in the gauche cyclopropyl group. However, we would like to point out that the predicted differences of as much as 0.012 Å for some of these bonds within a ring is undoubtedly a realistic difference.

Acknowledgment. J.R.D. acknowledges the University of Missouri−Kansas City for a Faculty Research Grant for partial financial support of this research. C.J.W. is grateful for the support provided by a development leave that allowed him to assist in carrying out this research.

Supporting Information Available: Table 1S, scaled diagonal force constants from MP2(full)/6-31G(d) ab initio calculations for 1,1-dicyclopropylethene; and Table 2S, symmetry coordinates of 1,1-dicyclopropylethylene. This material is available free of charge via the Internet at http://pubs.acs.org.

References and Notes

(1) Volltrauer, H. N.; Schwendeman, R. H. *J. Chem. Phys.* **1971**, *54*, 260.

(2) Bartell, L. S.; Guillory, J. P. *J. Chem. Phys.* **1965**, *43*, 647.

(3) Durig, J. R.; Bist, H. D.; Little, T. S. *J. Chem. Phys.* **1988**, *61*, 529.

(4) Durig, J. R.; Feng, F.; Little, T. S.; Wang, A. *Struct. Chem.* **1992**, *3*, 417.

(5) Durig, J. R.; Shen, S. *Spectrochim. Acta A* **2000**, *56*, 2545.

(6) Lüttke, W.; De Meijere, A. *Angew. Chem., Int. Ed. Engl.* **1966**, *5*, 512.

(7) Günther, H.; Wendisch, D. *Angew. Chem., Int. Ed. Engl.* **1966**, *5*, 251.

(8) De Mare, G. R.; Martin, J. S. *J. Am. Chem. Soc.* **1966**, *88*, 5033.

(9) Günther, H.; Klose, H.; Cremer, D. *Chem. Ber.* **1971**, *104*, 3884.

(10) De Meijere, A.; Lüttke, W. *Tetrahedron* **1969**, *25*, 2047.

(11) Hehre, W. J. *J. Am. Chem. Soc.* **1972**, *94*, 6592.

(12) Codding, E. G.; Schwendeman, R. H. *J. Mol. Spectrosc.* **1974**, *49*, 226.

(13) Carreira, L. A.; Towns, T. G.; Malloy, T. B., Jr. *J. Am. Chem. Soc.* **1978**, *100*, 385.

(14) Salares, V. R.; Murphy, W. F.; Bernstein, H. J. *J. Raman Spectrosc.* **1978**, *7*, 147.

(15) Wurrey, C. J.; Zheng, C.; Guirgis, G. A.; Durig, J. R. *Phys. Chem. Chem. Phys.* **2004**, *6*, 2125.

(16) Nease, A. B.; Wurrey, C. J. *J. Phys. Chem.* **1979**, *83*, 2135.

(17) Andrieu, C. G.; Paquer, D.; Mollier, Y. *C. R. Acad. Sci. Paris Ser. C* **1973**, *276*, 927.

(18) Aroney, M. J.; Calderbank, K. E.; Stootman, H. J. *J. Chem. Soc., Perkin Trans.* **1973**, *2*, 1365.

(19) Traetteberg, M.; Bakken, P.; Quesada, J. V.; Mastryukov, V. S.; Boggs, J. E. *J. Mol. Struct.* **1999**, *485/486*, 73.

(20) Durig, J. R.; Yu, Z.; Zheng, C.; Guirgis, G. A. *J. Phys. Chem. A* **2004**, *108*, 5353.

(21) Durig, J. R.; Shen, S.; Zhu, X.; Wurrey, C. J. *J. Mol. Struct.* **1999**, *485*, 501.

(22) Wurrey, C. J.; Shen, S.; Gounev, T. K.; Durig, J. R. J. *Mol. Struct.* **1997**, *405*, 207.

(23) Wurrey, C. J.; Shen, S.; Zhu. X.; Zhen, H.; Durig, J. R. *J. Mol. Struct.* **1998**, *449*, 203.

(24) Guirgis, G. A.; Wurrey, C. J.; Yu, Z.; Zhu, X.; Durig, J. R. *J. Phys. Chem. A* **1999**, *103*, 1509.

(25) Frisch, M. J.; Trucks, G. W.; Schlegel, H. B.; Scuseria, G. E.; Robb, M. A.; Cheeseman, J. R.; Montgomery, J. A., Jr.; Vreven, T.; Kudin, K. N.; Burant, J. C.; Millam, J. M.; Iyengar, S. S.; Tomasi, J.; Barone, V.; Mennucci, B.; Cossi, M.; Scalmani, G.; Rega, N.; Petersson, G. A.; Nakatsuji, H.; Hada, M.; Ehara, M.; Toyota, K.; Fukuda, R.; Hasegawa, J.; Ishida, M.; Nakajima, T.; Honda, Y.; Kitao, O.; Nakai, H.; Klene, M.; Li, X.; Knox, J. E.; Hratchian, H. P.; Cross, J. B.; Adamo, C.; Jaramillo, J.; Gomperts, R.; Stratmann, R. E.; Yazyev, O.; Austin, A. J.; Cammi, R.; Pomelli, C.; Ochterski, J. W.; Ayala, P. Y.; Morokuma, K.; Voth, G. A.; Salvador, P.; Dannenberg, J. J.; Zakrzewski, V. G.; Dapprich, S.; Daniels, A. D.; Strain, M. C.; Farkas, O.; Malick, D. K.; Rabuck, A. D.; Raghavachari, K.; Foresman, J. B.; Ortiz, J. V.; Cui, Q.; Baboul, A. G.; Clifford, S.; Cioslowski, J.; Stefanov, B. B.; Liu, G.; Liashenko, A.; Piskorz, P.; Komaromi, I.; Martin, R. L.; Fox, D. J.; Keith, T.; Al-Laham, M. A.; Peng, C. Y.; Nanayakkara, A.; Challacombe, M.; Gill, P. M. W.; Johnson, B.; Chen, W.; Wong, M. W.; Gonzalez, C.; Pople, J. A. *Gaussian 03*, revision B.04; Gaussian, Inc.: Pittsburgh, PA, 2003.

(26) Pulay, P. *Mol. Phys.* **1969**, *17*, 197.

(27) Guirgis, G. A.; Zhu, X.; Yu, Z.; Durig, J. R. *J. Phys. Chem. A* **2000**, *104*, 4383.

(28) Frisch, M. J.; Yamaguchi, Y.; Gaw, J. F.; Schaefer, H. F., III; Binkley, J. S. *J. Chem. Phys.* **1986**, *84*, 531.

(29) Amos, R. D. *Chem. Phys. Lett.* **1986**, *124*, 376.

(30) Polavarapu, P. L. *J. Phys. Chem.* **1990**, *94*, 8106.

(31) Chantry, G. W. In *The Raman Effect*; Anderson, A., Ed.; Marcel Dekker Inc.: New York, 1971; Vol. 1, Chapter 2.

(32) Dewar, M. J. S.; Fonken, G. J.; Jones, T. B.; Minter, D. E. *J. Chem. Soc., Perkin Trans.* **1976**, *2*, 764.

(33) Sugawara, Y.; Konaka, S.; Tamagawa, T.; Kimura, M. *Symposium on Molecular Structures*, October 1979, Tokyo, Japan.

(34) Takeshita, K. *J. Mol. Struct.* **1985**, *133*, 161.

(35) Bulanin, M. O. *J. Mol. Struct.* **1973**, *19*, 59.

(36) Van der Veken, B. J.; DeMunck, F. R. *J. Chem. Phys.* **1992**, *97*, 3060.

(37) Herrebout, W. A.; Van der Veken, B. J.; Wang, A.; Durig, J. R. J. *Phys. Chem.* **1995**, *99*, 578.

(38) Bulanin, M. O. *J. Mol. Struct.* **1995**, *347*, 73.

(39) Herrebout, W. A.; Van der Veken, B. J. *J. Phys. Chem.* **1996**, *100*, 9671.

(40) Traetteberg, M.; Bakken, P.; Almenningen, A.; Lüttke, W. *J. Mol. Struct.* **1988**, *189*, 357.

(41) Durig, J. R.; Zheng, C.; Warren, R. D.; Groner, P.; Wurrey, C. J.; Gounev, T. K. *J. Phys. Chem. A* **2003**, *107*, 7713.